ORIGINAL RESEARCH

DPS1 regulates cuticle development and leaf senescence in rice

Syed Adeel Zafar[1] [ID] | Muhammad Uzair[1] | Muhammad Ramzan Khan[2] | Suyash B. Patil[1] |
Jingjing Fang[1] | Jinfeng Zhao[1] | Sneh Lata Singla-Pareek[3] | Ashwani Pareek[4] [ID] |
Xueyong Li[1] [ID]

[1]National Key Facility for Crop Gene Resources and Genetic Improvement, Institute of Crop Sciences, Chinese Academy of Agricultural Sciences, Beijing, China

[2]National Institute for Genomics and Advanced Biotechnology, National Agricultural Research Centre, Islamabad, Pakistan

[3]Plant Stress Biology, International Centre for Genetic Engineering and Biotechnology, New Delhi, India

[4]Stress Physiology and Molecular Biology Laboratory, School of Life Sciences, Jawaharlal Nehru University, New Delhi, India

Correspondence
Xueyong Li, National Key Facility for Crop Gene Resources and Genetic Improvement, Institute of Crop Sciences, Chinese Academy of Agricultural Sciences, Beijing, China.
E-mail: lixueyong@caas.cn

Funding information
National Key R&D Program of China: 2016YFD0100401; National Major Project for Developing New GM Crops, Grant/Award Number: 2016ZX08009-003; Agricultural Science and Technology Innovation Program of Chinese Academy of Agricultural Sciences

Abstract

Leaves are the primary food-producing organs for a plant that carry out photosynthesis and contribute to biomass and grain yield. Leaf senescence is a developmentally regulated physiological process but early leaf senescence is known to negatively affect plant yield. The cuticle is an outer waxy protective layer on the leaf surface which protects plants from pathogens attack as well as dehydration. Our understanding of the molecular mechanisms underlying cuticle development and leaf senescence is still immature. The present study reports the role of the *DEGENERATED PANICLE AND PARTIAL STERILITY 1* (*DPS1*) gene encoding a cystathionine β-synthase (CBS) domain-containing protein in cuticle development and leaf senescence in rice. The *dps1* loss-of-function mutant showed leaf senescence phenotype with twisted leaves, significantly reduced chlorophyll content and degenerated chloroplasts characterized by a reduced number of starch granules and an abundance of osmiophilic bodies. Furthermore, *dps1* leaves displayed defective cuticle development, reduced wax and cutin compounds, and lower relative water content as compared with wild type. Physiological assays showed significantly higher accumulation of reactive oxygen species (ROS) accompanied by enhanced DNA fragmentation in *dps1* leaves, which could be associated with chloroplast degeneration and defective cuticle development. Transcriptome analysis revealed altered expression of several critical genes related to photosynthesis and wax/cutin pathway. This study revealed a crucial role of *DPS1* in regulating leaf cuticle development and senescence by affecting the expression of several genes. Thus, a moderate expression of *DPS1* is necessary for better plant growth and productivity.

KEYWORDS
cell death, chloroplast, cuticle, leaf senescence, reactive oxygen species, rice

1 | INTRODUCTION

Photosynthesis is a complex set of reactions taking place in all green-leaved plants. Enhancing photosynthesis has been reported as a crucial physiological strategy to increase the plant biomass and grain yield by increasing photosynthates allocation to sink tissues (seeds) (Parry et al., 2010; Wu et al., 2019). The green plants carry out photosynthesis by capturing the light energy from sunlight and converting it into chemical energy. This chemical energy is stored in the form of carbohydrates and transferred to other plant parts for their survival. This complex process of photosynthesis is carried out in the chlorophyll-containing cellular organelles, called chloroplasts. The green photosynthetic pigment chlorophyll directly absorbs the sunlight in blue and red regions of the spectrum and thus gives the green color to the leaves. Several rice mutants with spotted or albino leaves have been identified, which show defective chloroplast development and reduced chlorophyll (Niu et al., 2017; Ye et al., 2016). Leaf senescence is an essential developmental process that often leads to chloroplast degeneration and thus minimizes the process of photosynthesis (Niu et al., 2017; Sun et al., 2017). However, premature leaf senescence is a physiological abnormality that negatively affects the plant growth and final yield (Liang et al., 2014; Niu et al., 2017). Several genetic and environmental factors are also known to regulate leaf senescence and chloroplast degeneration in plants (Erdal, 2012; Tsai et al., 2019; Xu et al., 2006). For example, *ALBINIC LEAF AND GROWTH RETARDATION* (*ALR*) encodes a deoxycytidine monophosphate deaminase (dCMP deaminase or DCD) protein which catalyses the conversion of dCMP to dUMP (Niu et al., 2017). DCD maintains dNTP pool balance in a plant cell and plays a crucial role in healthy chloroplast development and cell death (Niu et al., 2017). Similarly, a chloroplast-localized thioredoxin m isoform (*Ostrxm*) plays a vital role in redox regulation of chloroplast target proteins involved in diverse physiological functions (Chi et al., 2008). Mutated *Ostrxm* protein resulted in various developmental defects in rice, including semi-dwarfism, pale-green leaves, abnormal chloroplast structure, and reduced carotenoid and chlorophyll content (Chi et al., 2008). Thus, chloroplast development is controlled via coordinated regulation of various genetic and environmental factors. For developing a complete understanding of this essential physiological trait, elucidation of the contributing genetic factors is a must.

Leaf shape is an important determinant of plant architecture and also affects the rate of photosynthesis (Xiong & Jiao, 2019). Leaves maintain their proper form due to the turgidity of cells by upholding the cellular water potential. In addition to being a physical barrier to pathogen entry, the cuticle plays a key role in avoiding water loss from the surface and thus maintains cellular turgidity fond leaf shape (Guo et al., 2019). Cuticle primarily consists of a cutin matrix made of

Δ-hydroxylated fatty acids, which is covered by epicuticular waxes (Martin et al., 2017). It thus plays a key role in drought tolerance in plants by avoiding or minimizing water loss (Guo et al., 2019; Qin et al., 2011). Cutin and wax are derived from fatty acid precursors. Cutin is composed of C16 and C18 hydroxy and epoxy–hydroxy fatty acid monomers. At the same time, waxes predominantly contain alcohols, aldehydes, ketones, alkanes, and esters derived from very-long-chain fatty acids (Buschhaus et al., 2007; Zafar, Patil, et al., 2020). Several genes controlling leaf cuticle development have been isolated in rice and some other plant species, which play a significant role in understanding the mechanism of cuticle development (Aharoni et al., 2004; Guo et al., 2019; Qin et al., 2011). However, further studies yielding the identification of new genes regulating leaf cuticle development in rice will further expand our understanding of the genetic and molecular mechanism of cuticle development in this important crop.

Reactive oxygen species (ROS) play diverse roles in plant development and stress responses. Higher levels of ROS can trigger programmed cell death (PCD) events at tissue and organ level, which may cause early leaf senescence (Loor et al., 2010). It is known that higher amounts of ROS are generated in defective and permeable cuticles under pathogen attack, which play a role in resistance against viral attack (Serrano et al., 2014; Survila et al., 2016). However, the role of ROS in regulating leaf cuticle development is not yet clear. We previously reported that *Degenerated Panicle and Partial Sterility 1* (*DPS1*) controls panicle apical degeneration and anther cuticle development by regulating ROS homeostasis (Zafar, Patil, et al., 2020). We revealed that *DPS1* was mainly expressed in anthers, large panicle and leaf blade while a weak expression was observed in other tissues. Further, DPS1 protein was found to be localized in mitochondria and interacts with specific thioredoxin proteins (Trx1 and Trx20) to regulate redox balance (Zafar, Patil, et al., 2020). Here, we report the role of *DPS1* in leaf senescence via regulating cuticle development in rice. This study improved our understanding of the role of *DPS1* gene in photosynthesis and leaf senescence thereby regulating final grain yield in rice.

2 | MATERIALS AND METHODS

2.1 | Plant materials and growth conditions

Rice mutant *dps1* was identified from an ethylmethane sulfonate-mutagenized M_2 population derived from the japonica rice cv. Shengdao 16. The unmutated cv. was used as wild type (WT) for phenotypic and physiological comparison. The *dps1* mutant was crossed with the *indica* variety Huanghuazhan for genetic analysis and gene mapping. All the parents, F_1 hybrids, F_2 population, and transgenic plants were grown in paddy fields

at Beijing, Shandong, and Hainan provinces under natural conditions with standard agronomic practices.

2.2 | Pigment analysis

Chlorophyll *a* and *b* concentrations were determined following the method of Arnon (1949). The equal amount of leaf tissues was immersed overnight in ethanol with gentle shaking. The absorbance of the extract was measured at 663 and 645 nm using a spectrophotometer (HITACHI, U2800) as described earlier (Zafar, Hameed, et al., 2020). Formulae for measurement of chlorophyll contents are here:

Concentration of chlorophyll a (mg/g F.W) = (12.7*A663) - (2.69*A645)

Concentration of chlorophyll b (mg/g F.W) = (22.9*A645) - (4.68*A663)

2.3 | Transmission electron microscopy

The particular leaf tissues of WT and *dps1* were harvested when the leaf-yellowing phenotype became evident, and fixed in 2.5% glutaraldehyde (pH 7.2) followed by vacuum infiltration. Subsequently, samples were successively washed three times with 0.2 mol/l sodium cacodylate buffer for 30 min, fixed in 10% osmic acid for one h, washed three times with deionized water for 45 min, dehydrated with ethanol, treated with acetone and embedded in epoxy resins, and polymerized at 70 °C. The samples were then cut into about 500–800 Å thick with an ultramicrotome (Leica EM UC7) and stained with the mixture of uranyl acetate dihydrate and lead citrate. The sections were washed with deionized water and visualized using a HITACHI Transmission Electron Microscope (HT7700).

2.4 | Scanning electron microscopy

For SEM analysis, leaves were fixed in 3.5% glutaraldehyde solution and then dehydrated through a graded ethanol series. The samples were dried by the critical-point drying method and sputter-coated with platinum, and then observed using a variable pressure scanning electron microscope (S3400 N, HITACHI) as described (Chun et al., 2020).

2.5 | Chlorophyll leaching assay

The chlorophyll leaching assay was performed as described before (Qin et al., 2011). The flag leaf was harvested from individual plants and cut into segments (about 3 cm) and immersed in 30 ml of 80% ethanol at room temperature with gentle shaking in the dark. At 0, 15, 30, 45, 60, 90, 120, and 180 min, 3 ml of extract was taken out for chlorophyll quantification, and the extract was poured back to the same tube after measurement. Measurements were performed in a relatively dark room with feeble light.

2.6 | Toluidine blue staining test

The toluidine blue (TB) staining was performed following a previously described method (Tanaka et al., 2004) with minor modifications. The leaves from 6 weeks old plants of WT and *dps1* mutant were harvested and immersed in 0.05% (w/v) toluidine blue solution for 1 h in dark. The leaves were then washed with distilled water 2–3 times to remove the excess toluidine blue solution from leaf surface and observed under stereomicroscope.

2.7 | Quantification of wax and cutin

Leaf tissues from the WT and *dps1* plants were collected at 6 weeks old stage when leaf yellowing and curling was obvious and photographed using a stereomicroscope to determine surface area. An equal volume of freeze-dried leaf material was then used to assess wax and cutin using GC-MS and GC-FID technique following the previously described protocol (Zhao et al., 2015).

2.8 | Vector construction and transformation

For complementation vector (*DPS1-gDNA-C*), complete genomic DNA fragment (9,685 bp) of *LOC_Os05 g32850* was amplified including 2-kb upstream region and 512-bp downstream region and cloned into the *Eco*RI and *Spe*I sites of the binary vector *pCAMBIA1305.1* using In-fusion HD cloning kit (Takara Bio USA, Inc.). For the overexpression vector (*DPS1-CDS-C*), the coding sequence (1587-bp) of *LOC_Os05 g32850* was cloned into the *Nco*I and *Spe*I sites of the *pCAMBIA 1305.1APFHC* vector under the control of rice *Actin 1* promoter. Promoter–*GUS* vector was constructed by cloning the *DPS1* promoter (2011-bp upstream region from start codon) into the *Eco*RI and *Nco*I sites of *pCAMBIA1305.1* vector. All the primer sequences used for vector construction are listed in Supplementary Table S1. After sequence confirmation, all the recombinant vectors were introduced into *Agrobacterium tumefaciens* strain EHA105 by electroporation and transformed into the *dps1* mutant callus except for the Promoter–*GUS* vector which was transformed into the callus of cv. Kitaake, as described earlier (Zafar, Patil, et al., 2020).

2.9 | TUNEL assay

TUNEL assay was performed as described earlier (Zafar, Patil, et al., 2020). Briefly, leaves at 6 weeks old stage were collected and fixed in FAA solution for 24 h followed by embedding in spur resin (DMAE, SPI, USA). Cross-sections of 1 μm were cut using an ultramicrotome (Leica EM UC7) and fixed on poly-L-lysine-coated glass slides (Sigma-Aldrich). The resin was then removed from glass slides using NaOH (2%) in absolute ethanol for 5 min. Slides containing sections were then hydrated using a graded ethanol series (100%, 90%, 85%, 75%, and 50%) and incubated with proteinase K working solution 20 μg/ml in 10 mM Tris/HCl, pH 7.4. TUNEL assay was further performed using the *In Situ* cell death detection kit, Fluorescein (Roche, Cat. no. 11684795910), following manufacturer instructions. The green fluorescence of fluorescein (TUNEL signal) and red fluorescence of propidium iodide were analyzed at 488 nm (excitation)/520 nm (detection), and 488 nm (excitation)/610 nm (detection), respectively, under a laser scanning confocal microscope (LSM 700; Carl Zeiss, Germany).

2.10 | Histochemical staining and quantitative measurement of ROS

DAB (3,3'-diaminobenzidine) and NBT (Nitroblue tetrazolium) staining were used to detect the accumulation of ROS, as described previously (Wu et al., 2019). Briefly, leaves from 6–7 weeks old plants of WT and *dps1* were infiltrated with 10 mM Tris–HCl (pH 6.5) containing 1 mg DAB (Sigma-Aldrich) per ml followed by incubation at 37 °C in the dark for 16 h. For NBT staining, leaves were infiltrated with 2 mg NBT per ml in 50 mM sodium phosphate buffer (pH 7.5) at 37 °C in the dark overnight. Tissues were then washed with bleaching solution (ethanol: acetic acid =3:1) to bleach out the chlorophyll at 60 °C for 30 min. Finally, the tissues were photographed using a stereomicroscope under uniform lighting.

ROS was measured quantitatively in terms of H_2O_2 from leaf extract of WT and *dps1* plants, as described earlier (Zafar, Hameed, et al., 2020). Briefly, 100 mg of fresh leaf tissues was harvested and ground to a fine powder with liquid nitrogen. The powder was extracted with 1 ml 50 mM sodium phosphate (pH 7.4) and incubated on ice for 20 min. The extracts were then centrifuged at 12,000 g for 15 min at 4 °C, and supernatant was used for quantification of H_2O_2 using the hydrogen peroxide assay kit (Beyotime, China, Cat no. S0038). The absorbance of the supernatant was measured at 560 nm, and H_2O_2 was calculated using standard curve as reported earlier (Zafar, Hameed, et al., 2020).

2.11 | Measurement of MDA

MDA (malondialdehyde) content was measured using the kit provided by Nanjing Jiancheng bioengineering Institute, China (Cat. no. A003), as described earlier (Zafar, Patil, et al., 2020). The leaf tissue extracts were prepared as mentioned above for H_2O_2, and the absorbance of the mixture was recorded at 532 nm.

2.12 | RNA sequencing

We performed whole-genome transcriptome analysis using RNA-sequencing approach. The WT and *dps1* mutant leaves were collected just at the start of leaf yellowing and twisting. Messenger RNA (mRNA) was extracted from three biological replicates and subjected to fragmentation for library preparation. After clustering, the libraries were sequenced on Illumina Hiseq X Ten platform using (2 × 150 bp) paired-end module. After filtering the raw reads, clean reads were mapped to the reference sequence by using HISAT2, and the alignment result was assessed to achieve the secondary quality control (D. Kim et al., 2019). The alignment files generated by HISAT2 were input to the Cufflinks software (Trapnell et al., 2012), which was a program for the comparative assembly of transcripts and the estimation of their abundance in a transcriptome sequencing experiment by using the measurement unit FPKM (Fragments Per Kilobase of transcript sequence per Millions of base pairs sequenced). The RNA-sequencing analysis was performed by "*ANNOROAD GENOME*." Heat maps representing differentially expressed genes (DEGs) between WT and *dps1* ($p < 0.05$) for particular metabolic processes were constructed using function heatmap in R package "pheatmap" (version 1.0.10). DEGs ($p < 0.05$) were mapped in KEGG to identify the genes involved in wax, cutin, and suberin biosynthesis pathway (dosa00073) in *dps1* (Kanehisa et al., 2006). Gene ontology was performed to identify the significantly enriched biological processes in *dps1* by using "The Gene Ontology Consortium" database (The Gene Ontology Consortium, 2017).

2.13 | RNA isolation and qRT-PCR

RNA was isolated from leaves using the RNAprep Pure Plant Kit (Beijing, China). One μg RNA was reverse transcribed into cDNA using HiScript II Q RT Supermix (Vazyme). ChamQ SYBR qPCR master mix (Vazyme) was used for the reaction, and qPCR was performed using an ABI Prism 7500 sequence detection system as described earlier (J. Zhao et al., 2017). *ACTIN1* and *Ubiquitin* genes were used as the internal control, and data were calculated using $2^{-\Delta\Delta Ct}$ method
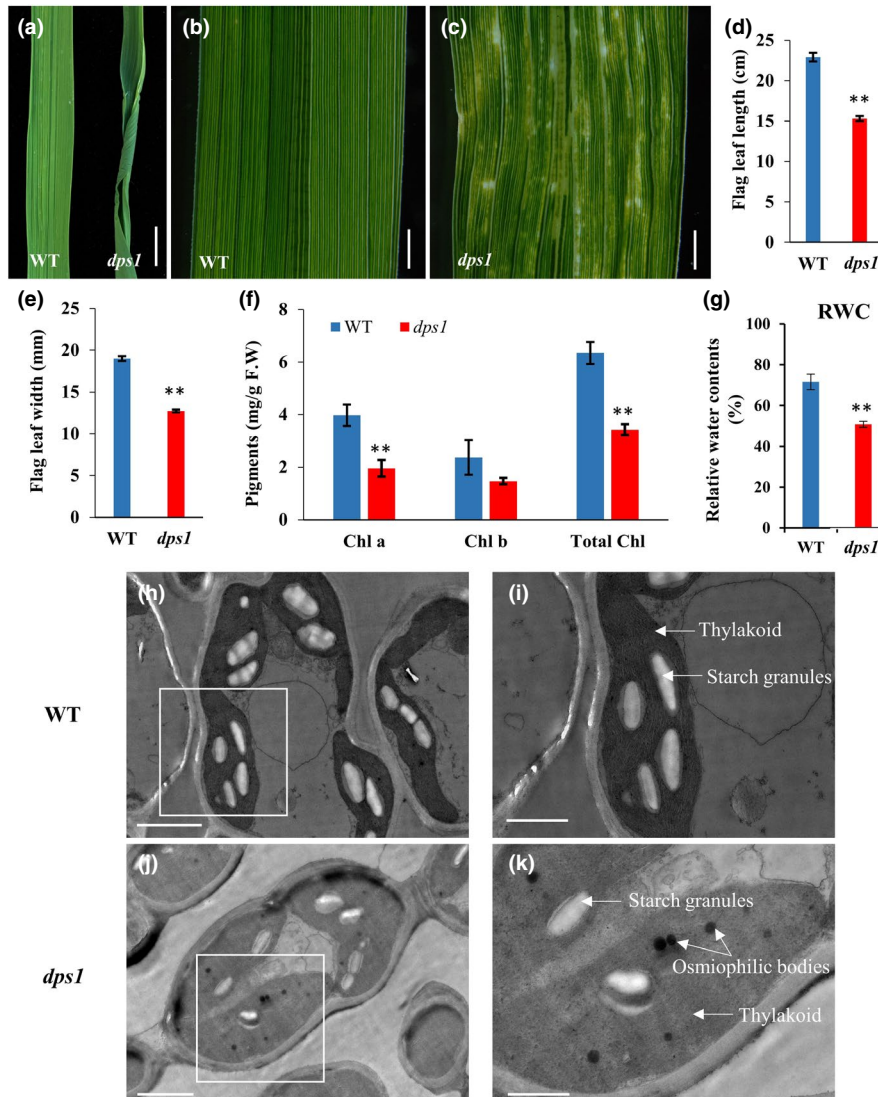
FIGURE 1 The *dps1* mutant has twisted yellow leaves and abnormal chloroplast development. Phenotypic analysis showing leaf twisting in the *dps1* mutant (a), normal green leaf in WT (b), and leaf having yellow patches in *dps1* (c). Quantitative analysis of flag leaf length (d) and width (e) in WT and *dps1*. Quantitative analysis of chlorophyll contents (f) and relative water content (g) in WT and *dps1* leaves. Data represent mean of 20 biological replicates in (d) and (e), and 5 biological replicates in (f) and (g). Significance of data in (d–g) is calculated with student's *t*-test. **$p < 0.01$. Transmission electron micrographs of chloroplast ultrastructure in WT (h) and *dps1* (j) leaves. (i) and (k) show enlarged view of the boxed region in (h) and (j), respectively. Arrows indicate the thylakoid, starch granules, and osmiophilic bodies. Chloroplast structure was observed from 3 biological repeats, and representative image is presented in (h) and (j). Scale bars: 1 cm (a), 2 mm (b and c), 20 μm (h and j), and 10 μm (i and k), respectively.

as described earlier (Livak & Schmittgen, 2001). All primer sequences used for qRT-PCR are listed in Supplementary table S2.

3 | RESULTS

3.1 | *DPS1* controls leaf senescence in rice

We previously reported that the *degenerated panicle and partial sterility 1* (*dps1*) mutant showed a partial fertility phenotype in rice (Zafar, Patil, et al., 2020). Here, we report

another novel phenotype of the *dps1* mutant, which is twisted yellow leaves having defective cuticle development. The *dps1* mutant showed healthy leaf development during early growth stages; however, it started to develop twisted flag leaves with patches of yellow color after five weeks of transplanting (WAT), and the phenotype became fully apparent after 6-WAT (Figure 1a-c and Supplementary Figure 1). The length and width of flag leaf were also significantly reduced in *dps1* as compared with WT (Figure 1d, e). Leaf yellowing is one of the most prominent features of senescence, which is usually due to the chlorophyll breakdown (Matile et al., 1996). We found significantly reduced chlorophyll a and total
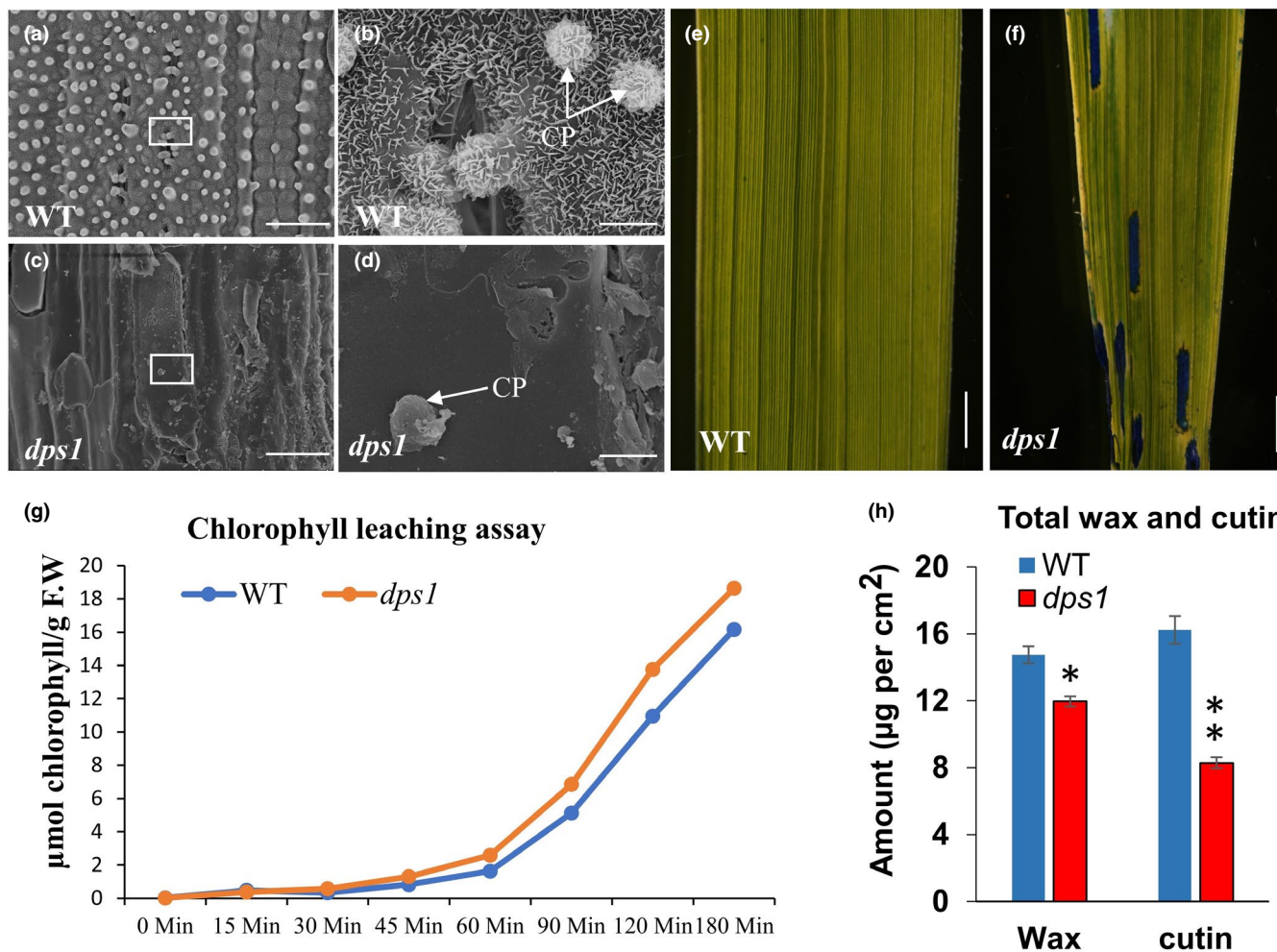
FIGURE 2 The *dps1* mutant showed defective cuticle and reduced wax and cutin compounds. Scanning electron micrographs for cuticle morphology in the WT (a) and *dps1* (c) leaves. (b) and (d) show enlarged view of (a) and (c), respectively. Box in (a) and (c) represent the region focused in (b) and (d), respectively. Leaf cuticle was observed from 3 biological repeats, and representative image is presented in (a) and (c). Toluidine blue staining for cuticle permeability in the WT (e) and *dps1* leaves (f). Representative image of toluidine blue staining observed from 3 independent plants is presented in (e) and (f). Chlorophyll leaching assay in the WT and *dps1* leaves (g). Analysis of total wax and cutin amounts in the WT and *dps1* leaves (h). Data represent mean of 5 biological repeats in (g), and 3 biological repeats in (h). Significance of data is calculated with student's *t*-test. *$p < 0.05$, **$p < 0.01$. Scale bars: 50 μm (a and c), 5 μm (b and d), 2 mm (e and f). CP; cuticular papillae.

chlorophyll contents in the *dps1* mutant compared with WT at 6-WAT (Figure 1f). Leaf relative water content (RWC) was also significantly reduced in *dps1* as compared with WT (Figure 1g). To confirm whether the decreased chlorophyll contents are due to leaf senescence, we also measured chlorophyll contents at 4-WAT when the leaf senescence and twisting phenotype did not occur. There was no significant difference in the chlorophyll contents among WT and the *dps1* mutant at early growth stage of 4-WAT (Supplementary Figure 2a). This indicated that chlorophyll reduction in *dps1* occured due to leaf senescence at later growth stages. To further elucidate the mechanism of leaf yellowing at the intracellular level, we observed the chloroplast ultrastructure from the yellow region of flag leaves using a transmission electron microscope (TEM). The WT leaves exhibited a typical chloroplast structure with well-developed thylakoid and

starch granules (Figure 1h, i). However, TEM showed abnormal thylakoid and a smaller number of improperly developed starch granules in *dps1* chloroplasts (Figure 1j, k). Notably, in contrast with WT, *dps1* chloroplasts had a large number of osmiophilic bodies (Figure 1k), which are a signal of disrupted chloroplast (Sun et al., 2017). These results indicate that changes in chlorophyll content and chloroplast structure are associated with leaf senescence. Since these changes are not seen before the induction of the senescence phenotype, this suggests that senescence lies upstream of these changes.

3.2 | *DPS1* controls leaf cuticle development

The cuticle is a key protecting covering on the leaf surface, which avoids excessive loss of water and maintains leaf
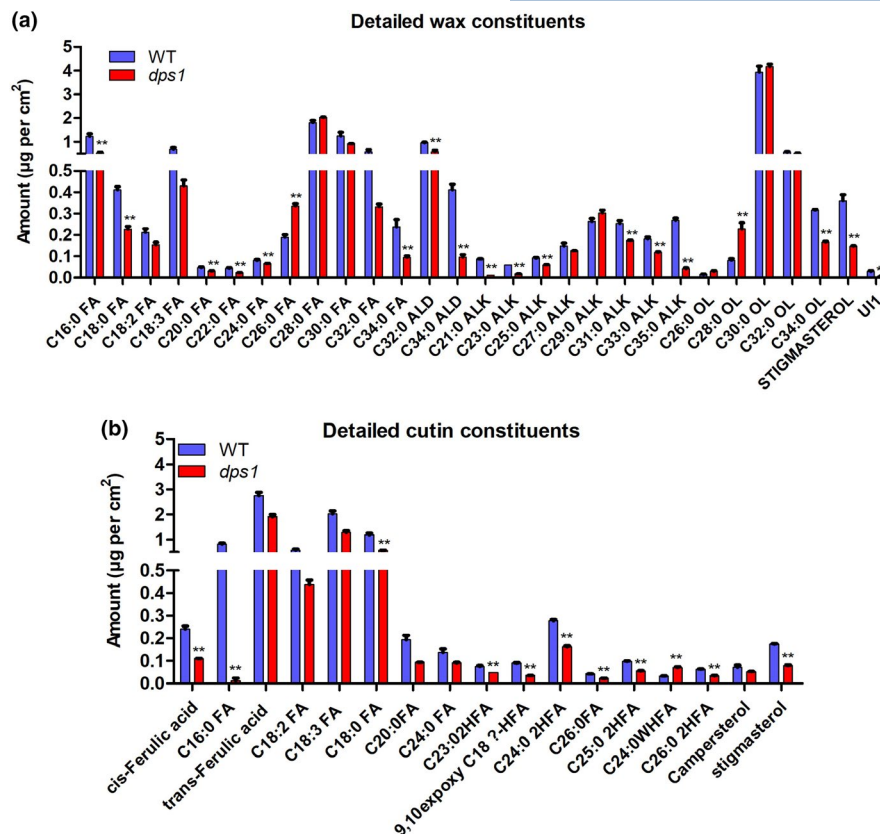
FIGURE 3 Detailed analysis of leaf wax and cutin compositions in WT and *dps1* by gas chromatography–mass spectrometry (GC-MS). Composition of wax constituents' amount (a) and amount of cutin monomers (b) per unit surface area (μg cm^{-2}) of the WT and *dps1* leaves. The values indicate mean of three biological replicates ± SE. Significance of data is calculated with student's *t*-test. **$p < 0.01$. Compound names are abbreviated as follows: FA, fatty acids; ALK, alkanes; OL, alcohols; C16:0 FA, palmitic acid; C18:0 FA, stearic acid; C18:2 FA, linoleic acid; C18:3 FA, linolenic acid; C20:0 FA, eicosanoic acid; C22:0 FA, docosanoic acid; C24:0 FA, tetracosanoic acid; C26:0 FA, cerotic acid; C28:0 FA, montanic acid; C30:0 FA, melissic acid; C32:0 FA, lacceroic acid; C34:0 FA, geddic acid; C16:0 ωHFA, 16-hydroxy-hexadecanoic acid; C18:1 ωHFA, 18-hydroxy-oleic acid; C18:2 ωHFA, 18-hydroxy-linoleic acid; cis-9,10-epoxy C18:0 ωHFA, cis-9,10-epoxy 18-hydroxy-stearic acid; cis-9,10-epoxy C18:1 ωHFA, cis-9,10-epoxy 18-hydroxy-oleic acid; C16-9/10 16 DHFA, 9(10), 16-dihydroxy-hexadecanoic acid; C18-9/10, 18 DHFA, 9(10),18-dihydroxy-stearic acid; C18:1–9/10, 18 DHFA, 9(10), 18-dihydroxy-oleic acid; C20 2HFA, 2-hydroxyeicosanoic acid; C20:0 DFA, eicosane-1, 20-dioic acid; C22:0 2HFA, 2-hydroxydocosanoic acid; C24:0 2HFA, 2-hydroxytetracosanoic acid.

shape. We thus hypothesized that leaf twisting in *dps1* could be due to absence or defective cuticle development. To test this hypothesis, we observed the leaf surface from WT and *dps1* for cuticle development using a scanning electron microscope (SEM). SEM observation indicated that WT leaves were covered by wax crystals and cuticular papillae (Figure 2a, b). However, we observed a smooth leaf surface without observable wax crystals and a few but naked cuticular papillae in the *dps1* mutant (Figure 2c, d). We then did toluidine blue (TB) staining, which has been used as an indicator of cuticle development (Tanaka et al., 2004). There was no TB staining in the WT leaves; however, apparent blue staining at particular leaf areas in the *dps1* mutant was observed at 6-WAT, indicating that cuticle was defective or absent in *dps1* at specific regions of the leaf which look yellow with the wrinkled surface (Figure 2e, f). To have further evidence about defective or missing cuticle, we did chlorophyll leaching assay, an indicator of cuticle permeability (Qin et al.,

2011). Chlorophyll leaching assay indicated a higher rate of chlorophyll removal from *dps1* leaves relative to the WT leaves (Figure 2g), suggesting a higher rate of cuticle permeability in *dps1*. These findings indicated that *dps1* leaves had defective cuticle development, particularly at specific regions, which caused an excessive loss of water, leading to leaf twisting. Notably, TB staning and chlorophyll leaching assays at early growth stage (before leaf senescence phenotype) showed no any difference between WT and *dps1*, suggesting that cuticle permeability was only affected after the leaf senescence started (Supplementary Figure 2b, c).

3.3 | Chemical analysis showed reduced wax and cutin compounds in *dps1*

To understand the exact reason for defective cuticle development in *dps1*, we did a detailed chemical analysis of wax

and cutin compounds, which are the major constituents of the leaf cuticle. Although both wax and cutin were significantly reduced in *dps1* leaves ($p < 0.05$ and $p < 0.01$, respectively), the reduction was more significant for cutin monomers as compared with wax (Figure 2h). Detailed analysis indicated

that, out of a total of 29 detected wax constituents, 17 were significantly reduced while 2 were increased dramatically in *dps1* leaves (Figure 3a). Regarding cutin monomers, although all components were decreased in *dps1* except C24:0 WHFA, a significant decrease was observed in 10 out of

**(k) Chlorophyll contents**

(l) RWC
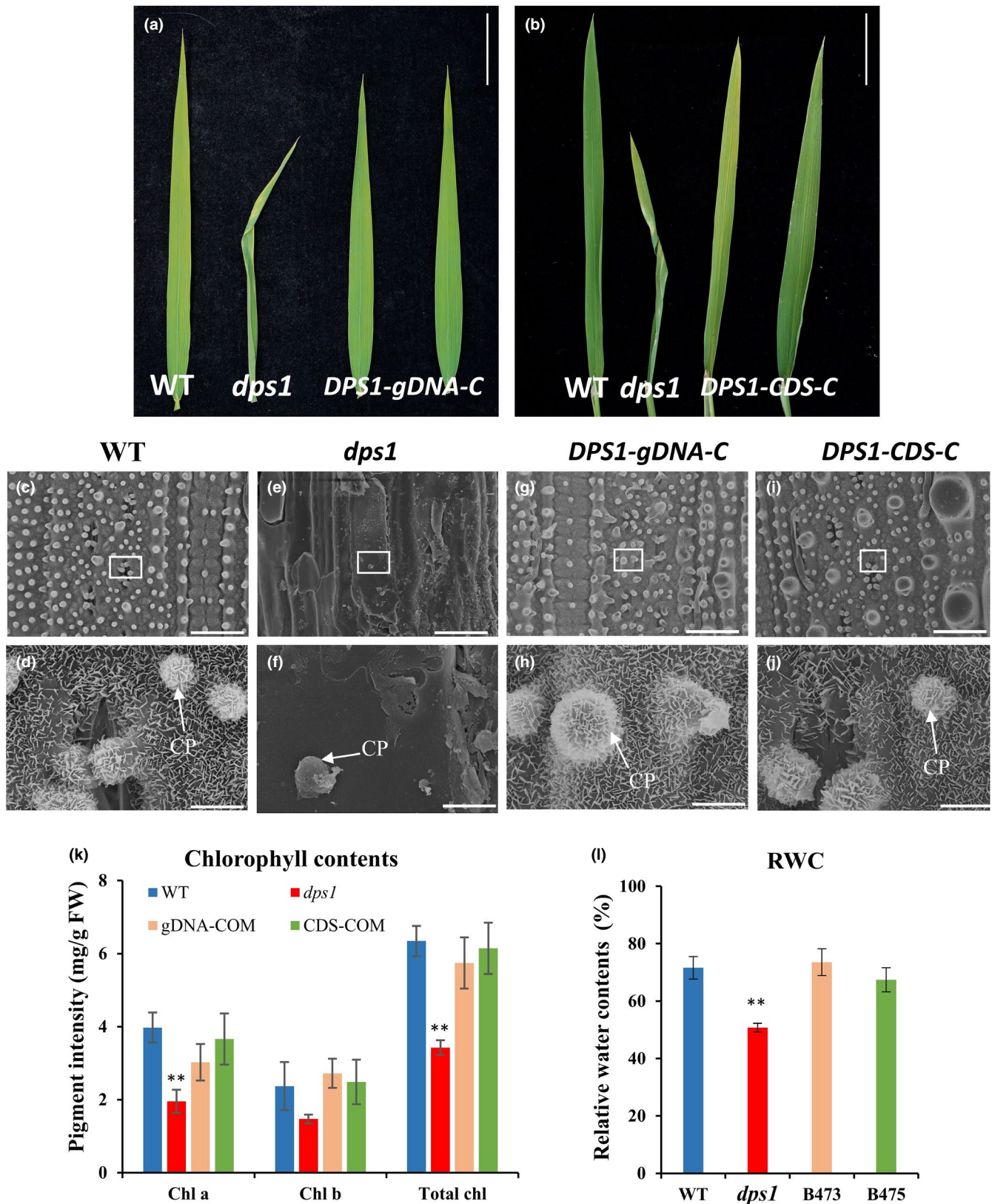
FIGURE 4 Genetic complementation of the leaf phenotype by *DPS1*. Flag leaves showing complementation of leaf phenotype in *DPS1-gDNA-C* plants (a) and *DPS1*-CDS overexpression plants (b). (c–j) Scanning electron micrographs showing complementation of leaf cuticle morphology in *DPS1-gDNA-C* plants and *DPS1*-CDS overexpression plants in comparison with WT and *dps1*. Scale bars: 5 cm (a and b), 50 μm (c, e, g, i), 5 μm (d, f, h, j). Box in (c, e, g, i) represents the region focused in (d, f, h, and j), respectively. (k) Pigment analysis showing genetic complementation of chlorophyll contents in *DPS1-gDNA-C* plants and *DPS1*-CDS overexpression plants in comparison with WT and *dps1*. (i) Complementation of relative water contents (RWC) in *DPS1-gDNA-C* plants (B473) and *DPS1*-CDS overexpression plants (B475) in comparison with WT and *dps1*. Data represent mean of 5 biological replicates, and significance of data is calculated with student's *t*-test. **$p < 0.01$. CP; cuticular papillae. The different phenotypic and physiological data shown were collected from the same transgenic lines.

17 components (Figure 3b). These findings indicated that mutation in *DPS1* influences leaf cuticle development and composition.

3.4 | Genetic complementation and expression pattern of *DPS1*

Our previous map-based cloning study confirmed that the degenerated panicle and partial sterility of the *dps1* mutant is caused by a loss-of-function mutation in *Os05 g0395300*

(known as *DPS1*) (Zafar, Patil, et al., 2020). To confirm whether the mutation in *Os05 g0395300* is also responsible for the leaf twisting, yellowing, and defective cuticle development in the *dps1* mutant, we performed transgenic complementation test by introducing the 9,685 bp wild type genomic DNA (gDNA) of *Os05 g0395300* into the *dps1* mutant. From the entire 28 transgenic lines (called hereafter *DPS1-gDNA-C*) obtained, 22 lines fully rescued the *dps1* mutant phenotype by showing healthy leaf development comparable with that of WT (Figure 4a). SEM examination also revealed healthy cuticle development on the
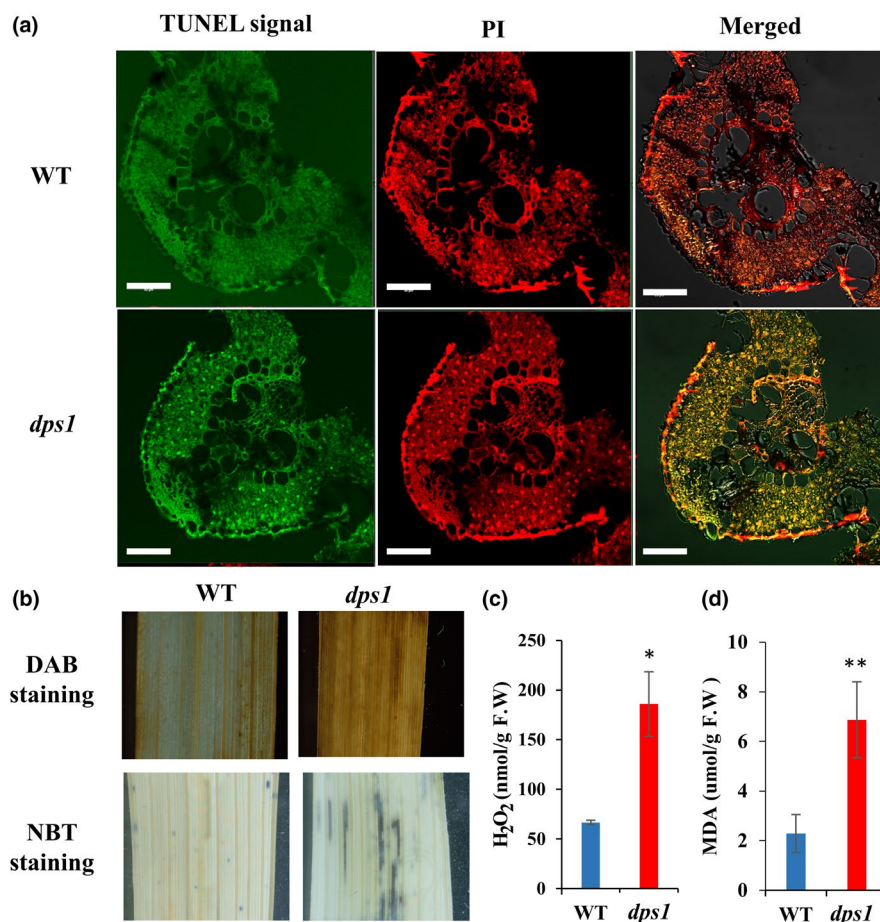
FIGURE 5 The *dps1* mutant leaves had enhanced DNA fragmentation and ROS accumulation. (a) *In situ* DNA fragmentation detection in the *dps1* leaf compared with WT by TUNEL assays. Green fluorescence indicates TUNEL positive signals for DNA fragmentation, red fluorescence indicates staining of leaves with propidium iodide (PI), and yellow fluorescence resulted from overlay of green signals of TUNEL and red signals of PI staining. Scale bars: 50 μm. (b) 3,3'-diaminobenzidine (DAB) and Nitroblue tetrazolium (NBT) staining of the WT and *dps1* leaves. (c) Increased H_2O_2 accumulation in the *dps1* leaves compared with WT. (d) Increased MDA level in the *dps1* leaves compared with WT. Data represent mean of 3 biological replicates. Significance of data is calculated with student's *t*-test. *$p < 0.05$, **$p < 0.01$.

DPS1-gDNA-C leaves similar with that of WT (Figure 4c-h). To further validate these data, we introduced the *DPS1* coding sequence expressed under the control of the rice *Actin 1* promoter (*DPS1-CDS-C*) into the *dps1* mutant. Consistently, this overexpression vector also restored the WT phenotype, giving almost similar results as of *DPS1-gDNA-C* plants (Figure 4b, i, j). We further tested if photosynthetic pigments in the transgenic complemented plants were also rescued. Both the *DPS1-gDNA-C* and *DPS1-CDS-C* transgenic plants showed a significant increase in leaf chlorophyll contents as compared with *dps1* (Figure 4k). The leaf RWC was also increased in the *DPS1-gDNA-C* and *DPS1-CDS-C* transgenic plants as compared with *dps1* (Figure 4l). The different kinds of phenotypic and physiological data shown in this work were collected from the same transgenic lines. Taken together, these results confirmed that *DPS1* controls leaf development and affects the photosynthetic pigments and cuticle biosynthesis.

To observe the expression pattern of *DPS1* throughout leaf development, we have fused the *GUS* gene under the *DPS1* promoter and transformed this *pDPS1-GUS* construct into a japonica rice variety Kitaake. Histochemical staining of the transgenic *pDPS1-GUS* plants revealed that *DPS1* showed no or little expression in leaf during the first three weeks after transplanting, but we observed increased expression at 4 and 5 WAT (Supplementary Figure 3). The qRT-PCR analysis showed somewhat consistent results and indicated that there was no or little expression of *DPS1* at 1 WAT, however a slightly increased expression at 3 WAT (Supplementary Figure 3). The expression was highest at 4 WAT, followed by 5 WAT.

3.5 | The *dps1* mutant leaves had enhanced cell death and ROS accumulation
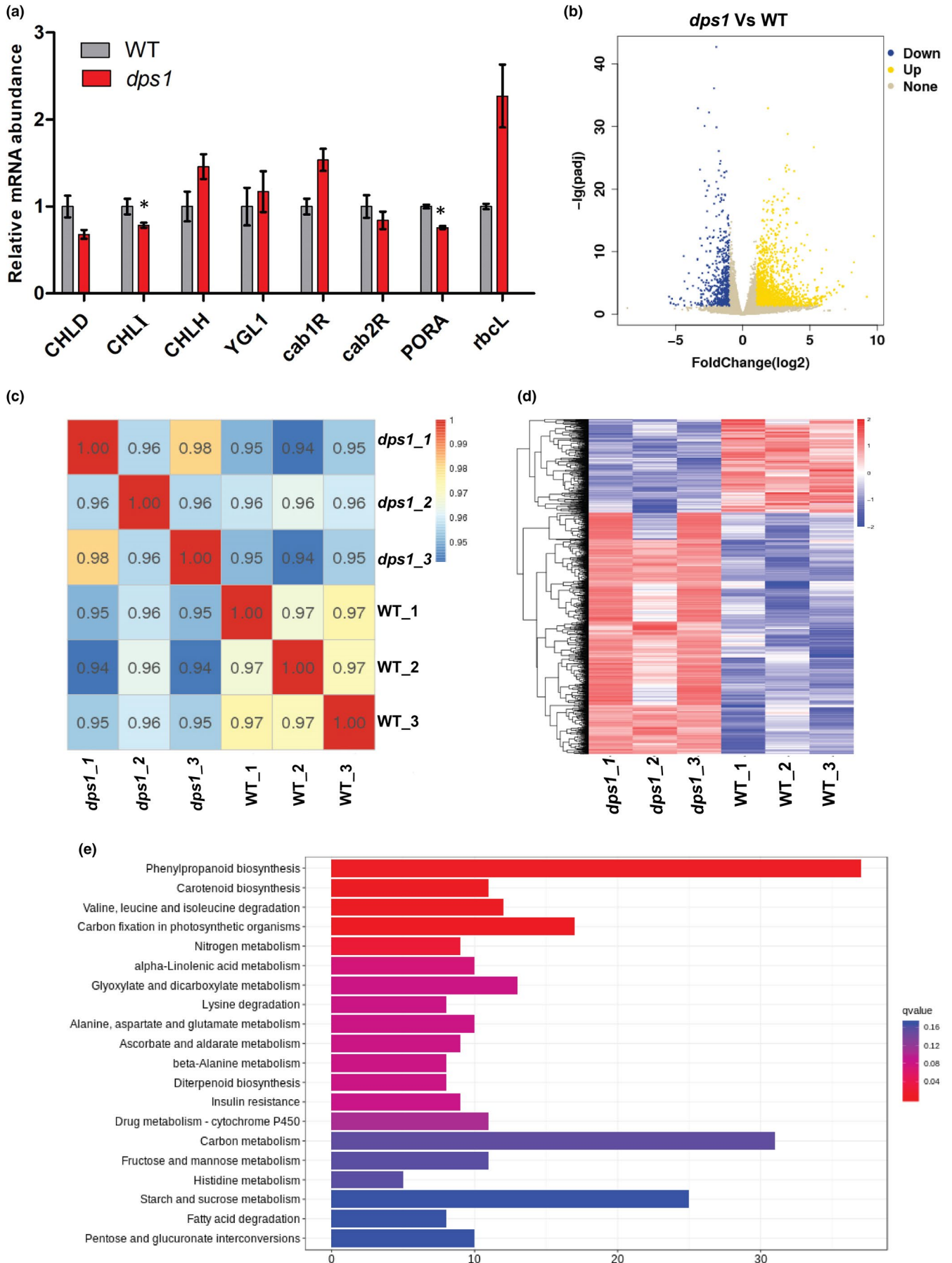
The yellow patches on the leaf surface showed a kind of leaf senescence phenotype. We thus hypothesized that this could be due to enhanced programmed cell death (PCD). Since PCD leads to DNA degradation, we compared the level of DNA fragmentation using the terminal deoxynucleotidyl transferase dUTP nick end labeling (TUNEL) assay, which indicates the amount of DNA fragmentation at a single cell level (Pu et al., 2017). In the TUNEL assay,

only few TUNEL-positive signals could be detected in WT, but a significantly higher amount of TUNEL-positive signals were detected in *dps1* leaves from 6 weeks old plants (Figure 5a), suggesting leaf senescence. Since ROS is an essential trigger of PCD, we tested if enhanced PCD in *dps1* leaves is due to elevated ROS levels. To test this hypothesis, we first did DAB and NBT staining to observe the accumulation of hydrogen peroxide (H_2O_2) and superoxide (O_2^-) in *dps1* leaves. We found higher staining of DAB and NBT in *dps1* leaves as compared with WT, suggesting a higher accumulation of ROS in *dps1* (Figure 5b). We further quantified the level of ROS and found a significantly higher ($p < 0.05$) amount of H_2O_2 in *dps1* leaves (Figure 5c). We also measured the levels of malondialdehyde (MDA), which is a marker for ROS-induced membrane lipid peroxidation (Zafar, Hameed, et al., 2020). A significantly higher ($p < 0.01$) level of MDA was observed in *dps1* leaves as compared with WT, suggesting ROS-induced damage in *dps1* (Figure 5d). Additionally, we also tested DAB and NBT staining in young leaves of WT and *dps1* before the appearance of leaf senescence phenotype which showed no obvious difference (staining) in leaves of either plants (Supplementary Figure 4). This indicates a possible correlation between leaf senescence and ROS level and suggests that cuticular damage results in leaf senescence leading to ROS accumulation.

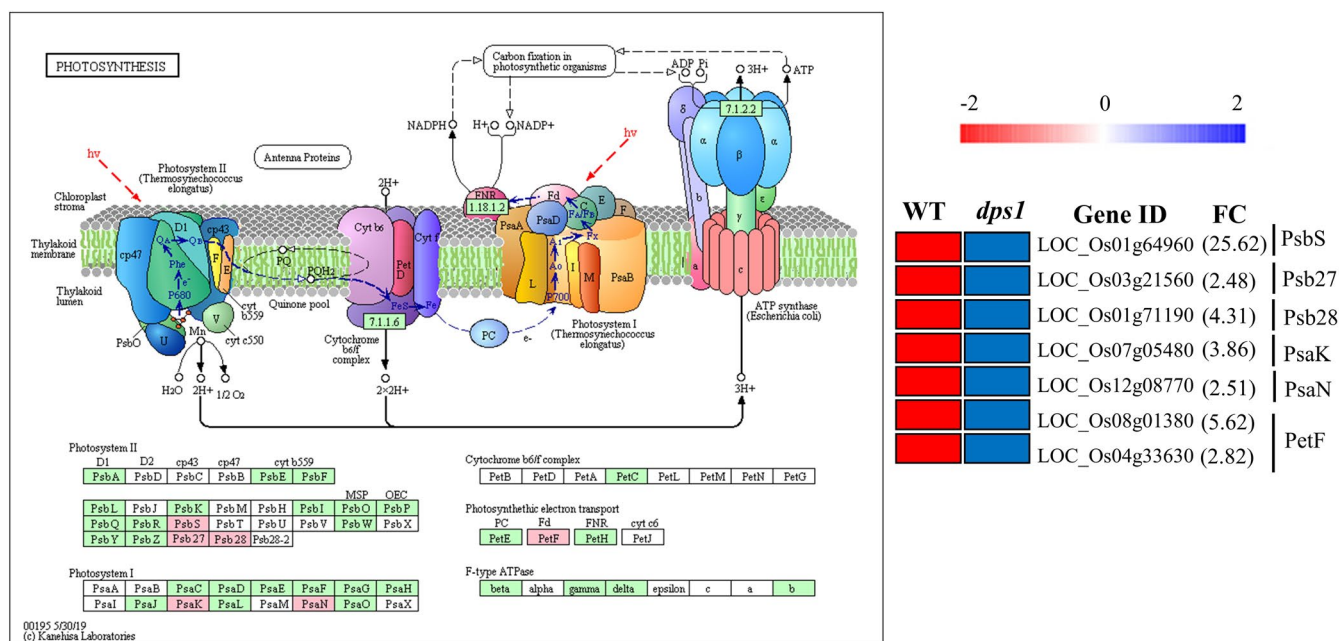## 3.6 | *DPS1* regulates expression of chloroplast biogenesis genes

To reveal the molecular basis of abnormal chloroplast development, we detected expression levels of previously reported genes involved in chloroplast or chlorophyll biogenesis using real-time quantitative PCR (qPCR). The expression of several genes related to chlorophyll biosynthesis, such as *CHLI* (encoding Mg-chelatase I subunit) and *PORA* (encoding NADPH-dependent protochlorophyllide oxidoreductase) (Armstrong et al., 1995; Zhang et al., 2006), was significantly reduced ($p < 0.05$) in *dps1* leaves compared with WT (Figure 6a). This suggests that defective chloroplast development causing leaf senescence in *dps1* could be due to reduced expression of *CHLD* (Mg-chelatase D subunit), *CHLI*, and *PORA*.

FIGURE 6 Global gene expression profiles of the WT and *dps1* leaves. (a) Relative expression of selected chloroplast-related genes in the (WT and *dps1* leaves by qRT-PCR. (b–e) Summary of transcriptome analysis between the WT and *dps1* leaves from RNA-seq analysis. (b) Overview of up- and downregulated genes between the WT and *dps1* leaves from RNA-seq analysis. (c) Correlation analysis between different samples of RNA-seq analysis of the WT and *dps1* leaves. (d) Heatmap showing expression pattern of differentially expressed genes between the WT and *dps1* leaves. (E) KEGG pathway analysis of differentially expressed genes between the WT and *dps1* leaves. RNA-seq and qRT-PCR data are mean ± SE of three biological repeats. Significance of data is calculated with student's *t*-test. *$p < 0.05$. *CHLD*, Mg-chelatase D subunit; *CHLI*, Mg-chelatase I subunit; *CHLH*, Mg-chelatase H subunit; *YGL1*, *Yellow*-*Green Leaf 1*; *Cab1R*, Chlorophyll a/b binding protein 1R; *Cab2R*, Chlorophyll a/b binding protein 2R; *PORA*, NADPH-dependent protochlorophyllide oxidoreductase; *rbcL*, Large subunit of Rubisco.

(a)

(b) *dps1* Vs WT

(c)

(d)

(e)

TABLE 1 Summary of transcriptome analysis. Values represent mean of three biological repeats.

Sample name	Total reads	Raw reads	Clean reads	Total mapped	Q30 (%)
WT	45,663,357	47334851	45663357	44145254	94
dps1	45,538,322	47734416	45538322	44029187	94

WT	*dps1*	Gene ID	FC	
		LOC_Os01g64960	(25.62)	PsbS
		LOC_Os03g21560	(2.48)	Psb27
		LOC_Os01g71190	(4.31)	Psb28
		LOC_Os07g05480	(3.86)	PsaK
		LOC_Os12g08770	(2.51)	PsaN
		LOC_Os08g01380	(5.62)	PetF
		LOC_Os04g33630	(2.82)	

FIGURE 7 Differentially expressed genes mapped to the photosynthesis pathway. The known pathway was obtained from the KEGG database. Green boxes show elements with known genes, red boxes show elements with DEGs, and white boxes show elements with unknown genes.

To get a more in-depth insight into the molecular mechanism of chloroplast development, we compared the global gene expression profile of the *dps1* mutant with its WT using RNA-sequencing (RNA-seq) approach. After filtering the raw reads from adapters and low-quality reads, we obtained a total of 45.5 GB clean reads with a quality score (Q30 rate) of 94%, indicating the high quality of Illumina sequencing (Table 1). We then obtained the expression levels of unigenes in terms of fragments per kb per million reads (FPKM) values. Compared with WT, expression of 1,727 unigenes was upregulated, while 671 unigenes were downregulated in *dps1* ($p < 0.05$) (Figure 6b, Data S1). The Pearson correlation analysis indicated a correlation of above 0.95 in all samples, which further showed the reliability of our sequencing dataset (Figure 6c). Heatmap based on FPKM values indicated that most of the genes were upregulated in *dps1* leaves as compared with WT (Figure 6d). Before proceeding for the downstream bioinformatics analysis, we have further validated the RNA-seq data by qRT-PCR analysis. We detected the relative mRNA level of seven randomly selected differentially expressed genes, six of which showed the same trend in qRT-PCR as in RNA-seq (FPKM values) (Supplementary Figure 5). This indicated that our RNA-seq data and its bioinformatics analysis were of sufficiently good quality.

To understand the molecular pathways contributed by these DEGs, we mapped these DEGs into the Kyoto Encyclopedia of Genes and Genomes (KEGG) database. The most significant biological pathways include phenylpropanoid biosynthesis, carotenoid biosynthesis, and carbon fixation in photosynthetic organisms (Figure 6e). Since all of these pathways were related to photosynthesis, it suggests that *DPS1* contributed to photosynthesis-related processes. To identify the critical DEGs involved in the photosynthesis pathway (dosa00195), the pathway most relevant to photosynthesis in KEGG, we further mapped the DEGs into this pathway. Strikingly, we found the increased expression of seven genes in *dps1* than WT involved in the photosynthesis pathway (Figure 7). *LOC_Os01 g64960* (encoding PsbS in the photosystem II) showed a 25-fold increase in *dps1* than WT. *LOC_Os03 g21560* and *LOC_Os01 g71190* (encoding Psb27 and Psb28, respectively, in the photosystem II) showed a 2.48- and 4.31-fold increase in *dps1* than WT. *LOC_Os07 g05480* and *LOC_Os12 g08770* encoding PsaK and PsaN, respectively, in the photosystem I showed more than 2.5-fold increase in *dps1* than WT. *LOC_Os08 g01380* and *LOC_Os04 g33630* encoding PetF from the photosynthetic electron transport showed a 5.62- and 2.82-fold increase in *dps1* than WT (Figure 7). These results suggest
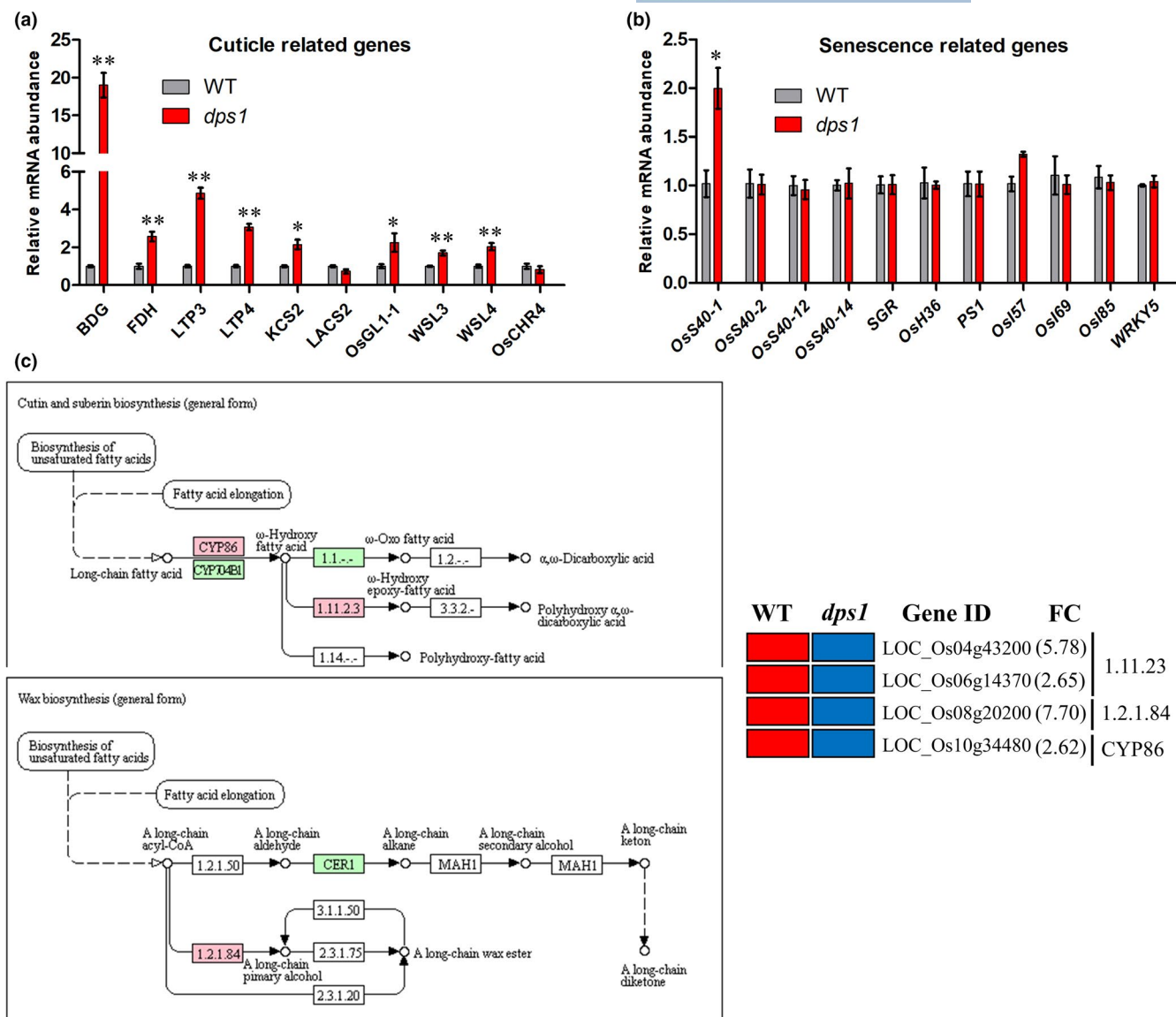
FIGURE 8 Expression profiles of leaf cuticle and senescence related genes. (a) Relative expression of 10 cuticle-associated genes in WT and *dps1* leaves using quantitative real-time PCR (qRT-PCR). Data are mean ± SE of three biological repeats. (b) Relative expression of 11 leaf senescence-associated genes in WT and *dps1* leaves using qRT-PCR. Data are mean ± SE of three biological repeats. Significance of data is calculated with student's *t*-test. *$p < 0.05$, **$p < 0.001$. (c) Differentially expressed genes mapped to the cutin, suberin, and wax biosynthesis pathway. The known pathway was obtained from the KEGG database. Green boxes show elements with known genes, red boxes show elements with DEGs, and white boxes show elements with unknown genes.

that increased expression of all seven DEGs in *dps1* from the photosynthesis pathway is probably a compensatory response due to the defective chloroplast development in these plants.

3.7 | *DPS1* regulates expression of cuticle-related genes

To understand the molecular basis of defective cuticle development, we detected expression levels of previously reported genes involved in cuticle biogenesis using qRT-PCR (Guo et al.,

2019; Qin et al., 2011; Tanaka et al., 2004). Surprisingly, we observed a significantly increased ($p < 0.01$) expression of several crucial cuticle biogenesis genes, namely, *BODYGUARD* (*BDG*), *FIDDLEHEAD* (*FDH*), *LIPID TRANSFER PROTEIN 3* (*LTP3*), *LIPID TRANSFER PROTEIN 4* (*LTP4*), *β-Ketoacyl-coenzyme A synthase 2* (*KCS2*), *Glossy1-1* (*OsGL1-1*), *Wax crystal-sparse leaf3* (*WSL3*), and *Wax crystal-sparse leaf4* (*WSL4*) in *dps1* than WT (Figure 8a). We further mapped all the DEGs into the "Cutin, suberin and wax biosynthesis" pathway, the most relevant KEGG pathway to cuticle biosynthesis (dosa00073). In agreement with our previous results of qRT-PCR (Figure 8a), we observed the upregulation of all four DEGs

detected in the cutin, suberin, and wax biosynthesis pathway in *dps1* compared with WT (Figure 8c). *LOC_Os04 g43200* (Caleosin related protein), *LOC_Os06 g14370* (Caleosin related protein), *LOC_Os08 g20200* (male sterility protein), and *LOC_Os10 g34480* (cytochrome P450 protein) showed 5.78-, 2.65-, 7.70-, and 2.62-fold increase in the expression in *dps1* as compared with WT (Figure 8c). These results indicate that *DPS1* is a crucial gene involved in cuticle development, and loss-of-function mutation in *DPS1* caused upregulation in the expression of other cuticle-associated genes, probably as a compensatory response to keep the development of cuticle in *dps1*.

3.8 | The senescence marker gene *OsS40-1* was upregulated in the *dps1* mutant

Leaf senescence is a precisely regulated process that involves specific expression of many senescence-associated genes (SAGs) (Liang et al., 2014). To see whether expression of SAGs is affected in the *dps1* mutant, we peformed qRT-PCR analysis of 11 different SAG genes (*OsS40-1*, *OsS40-2*, *OsS40-12*, *OsS40-14*, *OsWRKY5*, *PS1*, *SGR*, *Osh36*, *OsI57*, *Osh69*, and *OsI85*) in WT and *dps1*. According to our results, only *OsS40-1* was significantly upregulated in *dps1* compared with WT; however, the expression of other 10 SAG genes remained unchanged (Figure 8b). Since *OsS40-1* has been shown to be clearly upregulated under both natural and stress-induced leaf senescence (Zheng et al., 2019b) and that loss-of-function mutant of *DPS1* showed enhanced expression of *OsS40-1* (Figure 8b), our results suggest that defective cuticle development indeed led to the early leaf senescence in the *dps1* mutant.

4 | DISCUSSION

Leaf development is a genetically regulated process involving sophisticated cooperation of several genetic factors working in a single or multiple pathways (Xiong & Jiao, 2019). The chloroplast is a key cellular organelle responsible for food production for plants via photosynthesis. It captures light energy and converts carbon dioxide and water into oxygen and glucose, which are essential for plant and animal survival (Chi et al., 2008). Elucidating the mechanism of chloroplast development will improve our understanding of this complicated process. The present study reports that the leaf sensescence in the *dps1* mutant is correlated with reduced photosynthetic pigments due to chloroplast degeneration, enhanced cell death, and increased ROS level (Figures 1 and 5). Since chloroplast is an essential site for ROS production, we propose a possible correlation between chloroplast degeneration and elevated ROS level.

The cuticle is a vital covering on the leaf surface that protects plants from pathogen attack and excessive water loss (Qin et al., 2011; Serrano et al., 2014). Abnormal cuticle development usually leads to increased pathogens attack as well as susceptibility to drought (Guo et al., 2019; Serrano et al., 2014). In this study, the *dps1* mutant showed early leaf senescence accompanied by defective cuticle development on rice leaves (Figure 2). Our TB staining and chlorophyll leaching assays further confirmed the defective cuticle phenotype in *dps1* (Figure 2). The cuticle mainly consists of epicuticular wax and cutin ridges (Martin et al., 2017). Although a few genes regulating leaf cuticle development have been reported, its developmental and molecular mechanism is still not well understood (Aharoni et al., 2004; Guo et al., 2019; Qin et al., 2011). Our chemical analysis of wax and cutin monomers indicated that defective cuticle in *dps1* is due to significantly reduced cutin and wax components, and the role of cutin compounds was more as compared to wax (Figure 3). The leaf shape is sustained by the turgor pressure inside the cells, which is maintained by the water potential. The twisted leaf shape in *dps1* is probably due to excessive loss of water from the leaf surface as a result of defective cuticle development. It is possible that at a certain developmental stage, the lesion in cuticle biosynthesis becomes sufficiently severe to allow exposure of the leaf surface to the atmosphere resulting in extra stomatal water loss. Defective cuticle development may therefore be the trigger for leaf senescence from which downstream events such as ROS accumulation and chlorophyll loss begins.

ROS are important signaling molecules and regulate the expression of several genes (Hu et al., 2011; Zafar, Patil, et al., 2020). On the other side, overproduction of ROS is referred to as oxidative stress, which leads to damage of cellular organelles (Yu et al., 2017; Q. Zhao et al., 2018). We observed a higher DAB and NBT staining for ROS in the *dps1* mutant leaves, which was further confirmed by recording the significantly higher ROS levels in the *dps1* leaves (Figure 5). This higher ROS level was accompanied by enhanced PCD, as observed by TUNEL assay in the *dps1* leaves (Figure 5). Several studies have reported the ROS-mediated increased cell death in different vegetative and reproductive tissues (Dhindsa et al., 1981; Survila et al., 2016; Zheng, Li, et al., 2019). The defective cuticle development and reduced wax and cutin compounds in *dps1* may be correlated with enhanced PCD and ROS levels in leaf tissues.

To further study the molecular responses due to *DPS1* mutation, we analyzed the relative mRNA abundance of chloroplast development-related genes (Armstrong et al., 1995; Guo et al., 2019; Jung et al., 2003; Matsuoka, 1990; Niu et al., 2017; Zhang et al., 2006). From the eight genes studied, we observed significant downregulation in the expression of *CHLI* and *PORA*, genes related to chlorophyll biosynthesis (Armstrong et al., 1995; Zhang et al., 2006), suggesting

that these two genes could be downstream target genes of *DPS1*. Inversely, we observed significant upregulation in the expression of eight critical genes related to leaf cuticle development in *dps1* compared with WT (Guo et al., 2019; Qin et al., 2011; Tanaka et al., 2004), suggesting a robust compensatory response by the *dps1* mutant. Several senescence-associated genes (SAGs) have been identified that regulate the leaf senescence process (T. Kim et al., 2019; Liang et al., 2014; Zheng, Jehanzeb, et al., 2019). To see whether *DPS1* affects the expression of SAGs, we tested the relative mRNA abundance of 11 SAG genes in the *dps1* mutant and WT. We observed 2-fold upregulation in the expression of *OsS40-1* in *dps1* (Figure 8), an important SAG marker gene in rice (Zheng, Jehanzeb, et al., 2019), suggesting that *OsS40-1* is a downstream target gene of *DPS1*. Since ROS is an important signaling molecule for gene expression (Ribeiro et al., 2017; Zafar, Patil, et al., 2020), we studied global gene expression changes in *dps1* versus WT using RNA-seq analysis. We have identified 2,398 DEGs ($p < 0.05$) between *dps1* and WT, and most of the DEGs showed upregulation in *dps1* compared with WT (Figure 6). Mapping of these 2,398 DEGs in KEGG revealed the increased expression of seven genes in *dps1* than WT involved in the photosynthesis pathway (Figure 7). These genes were related to photosystem I, photosystem II, and electron transport chain. The increased expression of all seven DEGs in *dps1* in the photosynthesis pathway is probably a compensatory response as an evolutionarily stable strategy to continue at least minimum photosynthesis to sustain the plant growth (McNickle & Evans, 2018; Miller & Roath, 1982). To observe the molecular response in cuticle development, we mapped these 2,398 DEGs into the "Cutin, suberin, and wax biosynthesis" pathway of KEGG. Similarly, we observed the upregulation of all of the four DEGs in *dps1* compared with WT, suggesting again the compensatory response by mutant to maintain at least minimum levels of cuticle development (Figure 8). Recently, drought stress-induced changes in leaf cuticular wax composition and upregulation of cuticular wax-related genes have been reported in grape berry (Dimopoulos et al., 2020), which further suggest that loss of water from leaves due to defective cuticle may cause the upregulation of wax and cutin-associated genes in our study.

5 | CONCLUSION

Taken together, this study suggests that *DPS1* plays an essential role in leaf cuticle development and that mutation in *DPS1* results in early senescence that leads to ROS accumulation and chloroplast degeneration. Further, it also highlights the importance of compensatory response by the plant in the form of increased expression of several critical genes associated with a particular biological pathway after a genetic change/mutation in an essential structural or regulatory gene.

CONFLICT OF INTEREST

None declared.

AUTHORS' CONTRIBUTIONS

X.L. and S.A.Z. designed the experiments. S.A.Z. and M.U. performed most of the experiments. S.B.P., J.F., and J.Z. helped in data collection and provided technical assistance. S.A.Z., M.R.K., and A.P analyzed the data. S.A.Z. wrote the manuscript. S.A.Z., X.L., S.L.SP., and A.P. revised the manuscript. X.L. supervised the whole study.

ORCID

Syed Adeel Zafar https://orcid.org/0000-0002-4859-144X
Ashwani Pareek https://orcid.org/0000-0002-2923-0681
Xueyong Li https://orcid.org/0000-0002-8955-0345

REFERENCES

Aharoni, A., Dixit, S., Jetter, R., Thoenes, E., van Arkel, G., & Pereira, A. (2004). The SHINE clade of AP2 domain transcription factors activates wax biosynthesis, alters cuticle properties, and confers drought tolerance when overexpressed in Arabidopsis. *The Plant Cell*, *16*(9), 2463–2480. https://doi.org/10.1105/tpc.104.022897.

Armstrong, G. A., Runge, S., Frick, G., Sperling, U., & Apel, K. (1995). Identification of NADPH:protochlorophyllide oxidoreductases A and B: a branched pathway for light-dependent chlorophyll biosynthesis in Arabidopsis thaliana. *Plant Physiology*, *108*(4), 1505–1517. https://doi.org/10.1104/pp.108.4.1505.

Buschhaus, C., Herz, H., & Jetter, R. (2007). Chemical composition of the epicuticular and intracuticular wax layers on adaxial sides of Rosa canina leaves. *Annals of Botany*, *100*(7), 1557–1564. https://doi.org/10.1093/aob/mcm255.

Chi, Y. H., Moon, J. C., Park, J. H., Kim, H. S., Zulfugarov, I. S., Fanata, W. I., … Lee, S. Y. (2008). Abnormal chloroplast development and growth inhibition in rice thioredoxin m knock-down plants. *Plant Physiology*, *148*(2), 808–817. https://doi.org/10.1104/pp.108.123547.

Chun, Y., Fang, J., Zafar, S. A., Shang, J., Zhao, J., Yuan, S., & Li, X. (2020). MINI SEED 2 (MIS2) Encodes a receptor-like kinase that controls grain size and shape in rice. *Rice (N Y)*, *13*(1), 7. https://doi.org/10.1186/s12284-020-0368-9.

Dhindsa, R. S., Plumb Dhindsa, P., & Thorpe, T. A. (1981). Leaf senescence: correlated with increased levels of membrane

permeability and lipid peroxidation, and decreased levels of superoxide dismutase and catalase. *Journal of Experimental Botany*, *32*(1), 93–101.

Dimopoulos, N., Tindjau, R., Wong, D. C. J., Matzat, T., Haslam, T., Song, C., Gambetta, G. A., Kunst, L., & Castellarin, S. D. (2020). Drought stress modulates cuticular wax composition of the grape berry. *Journal of Experimental Botany*, *71*(10), 3126–3141. https://doi.org/10.1093/jxb/eraa046.

Erdal, S. (2012). Androsterone-induced molecular and physiological changes in maize seedlings in response to chilling stress. *Plant Physiology and Biochemistry*, *57*, 1–7. https://doi.org/10.1016/j.plaphy.2012.04.016.

Guo, T., Wang, D., Fang, J., Zhao, J., Yuan, S., Xiao, L., & Li, X. (2019). Mutations in the rice OsCHR4 gene, encoding a CHD3 family chromatin remodeler, induce narrow and rolled leaves with increased cuticular wax. *International Journal of Molecular Sciences*, *20*(10), https://doi.org/10.3390/ijms20102567.

Hu, L., Liang, W., Yin, C., Cui, X., Zong, J., Wang, X., Hu, J., & Zhang, D. (2011). Rice MADS3 regulates ROS homeostasis during late anther development. *The Plant Cell*, *23*(2), 515–533. https://doi.org/10.1105/tpc.110.074369.

Jung, K. H., Hur, J., Ryu, C. H., Choi, Y., Chung, Y. Y., Miyao, A., Hirochika, H., & An, G. (2003). Characterization of a rice chlorophyll-deficient mutant using the T-DNA gene-trap system. *Plant and Cell Physiology*, *44*(5), 463–472. https://doi.org/10.1093/pcp/pcg064.

Kanehisa, M., Goto, S., Hattori, M., Aoki-Kinoshita, K. F., Itoh, M., Kawashima, S., … Hirakawa, M. (2006). From genomics to chemical genomics: new developments in KEGG. *Nucleic Acids Research*, *34*(Database issue), D354–D357. https://doi.org/10.1093/nar/gkj102.

Kim, D., Paggi, J. M., Park, C., Bennett, C., & Salzberg, S. L. (2019). Graph-based genome alignment and genotyping with HISAT2 and HISAT-genotype. *Nature Biotechnology*, *37*(8), 907–915. https://doi.org/10.1038/s41587-019-0201-4.

Kim, T., Kang, K., Kim, S.-H., An, G., & Paek, N.-C. (2019). OsWRKY5 promotes rice leaf senescence via senescence-associated NAC and abscisic acid biosynthesis pathway. *International Journal of Molecular Sciences*, *20*(18), 4437. https://doi.org/10.3390/ijms20184437.

Liang, C., Wang, Y., Zhu, Y., Tang, J., Hu, B., Liu, L., Ou, S., Wu, H., Sun, X., Chu, J., & Chu, C. (2014). OsNAP connects abscisic acid and leaf senescence by fine-tuning abscisic acid biosynthesis and directly targeting senescence-associated genes in rice. *Proceedings of the National Academy of Sciences of the United States of America*, *111*(27), 10013–10018. https://doi.org/10.1073/pnas.1321568111.

Livak, K. J., & Schmittgen, T. D. (2001). Analysis of relative gene expression data using real-time quantitative PCR and the 2−ΔΔCT method. *Methods*, *25*(4), 402–408. https://doi.org/10.1006/meth.2001.1262.

Loor, G., Kondapalli, J., Schriewer, J. M., Chandel, N. S., Vanden Hoek, T. L., & Schumacker, P. T. (2010). Menadione triggers cell death through ROS-dependent mechanisms involving PARP activation without requiring apoptosis. *Free Radical Biology and Medicine*, *49*(12), 1925–1936. https://doi.org/10.1016/j.freeradbiomed.2010.09.021.

Martin, L. B. B., Romero, P., Fich, E. A., Domozych, D. S., & Rose, J. K. C. (2017). Cuticle biosynthesis in tomato leaves Is developmentally regulated by abscisic acid. *Plant Physiology*, *174*(3), 1384–1398. https://doi.org/10.1104/pp.17.00387.

Matile, P., Hortensteiner, S., Thomas, H., & Krautler, B. (1996). Chlorophyll breakdown in senescent leaves. *Plant Physiology*, *112*(4), 1403.

Matsuoka, M. (1990). Classification and characterization of cDNA that encodes the light-harvesting chlorophyll a/b binding protein of photosystem II from rice. *Plant and Cell Physiology*, *31*(4), 519–526. https://doi.org/10.1093/oxfordjournals.pcp.a077940.

McNickle, G. G., & Evans, W. D. (2018). Toleration games: compensatory growth by plants in response to enemy attack is an evolutionarily stable strategy. *AoB PLANTS*, *10*(4), ply035-ply035. https://doi.org/10.1093/aobpla/ply035.

Miller, J. F., & Roath, W. W. (1982). Compensatory response of sunflower to stand reduction applied at different plant growth stages1. *Agronomy Journal*, *74*(1), 119–121. https://doi.org/10.2134/agronj1982.00021962007400010030x.

Niu, M., Wang, Y., Wang, C., Lyu, J., Wang, Y., Dong, H., Long, W., Wang, D., Kong, W., Wang, L., Guo, X., Sun, L., Hu, T., Zhai, H., Wang, H., & Wan, J. (2017). ALR encoding dCMP deaminase is critical for DNA damage repair, cell cycle progression and plant development in rice. *Journal of Experimental Botany*, *68*(21–22), 5773–5786. https://doi.org/10.1093/jxb/erx380.

Parry, M. A. J., Reynolds, M., Salvucci, M. E., Raines, C., Andralojc, P. J., Zhu, X.-G., & Furbank, R. T. (2010). Raising yield potential of wheat. II. Increasing photosynthetic capacity and efficiency. *Journal of Experimental Botany*, *62*(2), 453–467. https://doi.org/10.1093/jxb/erq304.

Pu, C.-X., Han, Y.-F., Zhu, S., Song, F.-Y., Zhao, Y., Wang, C.-Y., & Sun, Y. (2017). The rice receptor-like kinases DWARF AND RUNTISH SPIKELET1 and 2 repress cell death and affect sugar utilization during reproductive development. *The Plant Cell*, *29*(1), 70–89. https://doi.org/10.1105/tpc.16.00218.

Qin, B. X., Tang, D., Huang, J., Li, M., Wu, X. R., Lu, L. L., & Cheng, Z. K. (2011). Rice OsGL1-1 is involved in leaf cuticular wax and cuticle membrane. *Molecular Plant*, *4*(6), 985–995. https://doi.org/10.1093/mp/ssr028.

Ribeiro, C. W., Korbes, A. P., Garighan, J. A., Jardim-Messeder, D., Carvalho, F. E. L., Sousa, R. H. V., Caverzan, A., Teixeira, F. K., Silveira, J. A. G., & Margis-Pinheiro, M. (2017). Rice peroxisomal ascorbate peroxidase knockdown affects ROS signaling and triggers early leaf senescence. *Plant Science*, *263*, 55–65. https://doi.org/10.1016/j.plantsci.2017.07.009.

Serrano, M., Coluccia, F., Torres, M., L'Haridon, F., & Metraux, J. P. (2014). The cuticle and plant defense to pathogens. *Frontiers in Plant Science*, *5*, 274. https://doi.org/10.3389/fpls.2014.00274.

Sun, L., Wang, Y., Liu, L. L., Wang, C., Gan, T., Zhang, Z. , Wang, Y., Wang, D., Niu, M., Long, W., Li, X., Zheng, M., Jiang, L., & Wan, J. (2017). Isolation and characterization of a spotted leaf 32 mutant with early leaf senescence and enhanced defense response in rice. *Scientific Reports*, *7*, 41846. https://doi.org/10.1038/srep41846.

Survila, M., Davidsson, P. R., Pennanen, V., Kariola, T., Broberg, M., Sipari, N., Heino, P., & Palva, E. T. (2016). Peroxidase-generated apoplastic ROS impair cuticle integrity and contribute to DAMP-elicited defenses. *Frontiers in Plant Science*, *7*, 1945. https://doi.org/10.3389/fpls.2016.01945.

Tanaka, T., Tanaka, H., Machida, C., Watanabe, M., & Machida, Y. (2004). A new method for rapid visualization of defects in leaf cuticle reveals five intrinsic patterns of surface defects in Arabidopsis. *The Plant Journal*, *37*(1), 139–146. https://doi.org/10.1046/j.1365-313X.2003.01946.x.

Trapnell, C., Roberts, A., Goff, L., Pertea, G., Kim, D., Kelley, D. R., & Pachter, L. (2012). Differential gene and transcript expression analysis of RNA-seq experiments with TopHat and Cufflinks. *Nature Protocols*, 7(3), 562–578. https://doi.org/10.1038/nprot.2012.016.

Tsai, Y. C., Chen, K. C., Cheng, T. S., Lee, C., Lin, S. H., & Tung, C. W. (2019). Chlorophyll fluorescence analysis in diverse rice varieties reveals the positive correlation between the seedlings salt tolerance and photosynthetic efficiency. *BMC Plant Biology*, 19(1), 403. https://doi.org/10.1186/s12870-019-1983-8.

Wu, A., Hammer, G. L., Doherty, A., von Caemmerer, S., & Farquhar, G. D. (2019). Quantifying impacts of enhancing photosynthesis on crop yield. *Nature Plants*, 5(4), 380–388. https://doi.org/10.1038/s41477-019-0398-8.

Xiong, Y., & Jiao, Y. (2019). The diverse roles of auxin in regulating leaf development. *Plants*, 8(7), 243.

Xu, S., Li, J., Zhang, X., Wei, H., & Cui, L. (2006). Effects of heat acclimation pretreatment on changes of membrane lipid peroxidation, antioxidant metabolites, and ultrastructure of chloroplasts in two cool-season turfgrass species under heat stress. *Environmental and Experimental Botany*, 56(3), 274–285.

Ye, W., Hu, S., Wu, L., Ge, C., Cui, Y., Chen, P., Wang, X., Xu, J., Ren, D., Dong, G., Qian, Q., & Guo, L. (2016). White stripe leaf 12 (WSL12), encoding a nucleoside diphosphate kinase 2 (OsNDPK2), regulates chloroplast development and abiotic stress response in rice (Oryza sativa L.). *Molecular Breeding*, 36, 57. https://doi.org/10.1007/s11032-016-0479-6.

Yu, S.-X., Feng, Q.-N., Xie, H.-T., Li, S., & Zhang, Y. (2017). Reactive oxygen species mediate tapetal programmed cell death in tobacco and tomato. *BMC Plant Biology*, 17(1), 76. https://doi.org/10.1186/s12870-017-1025-3.

Zafar, S. A., Hameed, A., Ashraf, M., Khan, A. S., Qamar, Z. U., Li, X., & Siddique, K. H. M. (2020). Agronomic, physiological and molecular characterisation of rice mutants revealed the key role of reactive oxygen species and catalase in high-temperature stress tolerance. *Functional Plant Biology*, 47(5), 440–453. https://doi.org/10.1071/fp19246.

Zafar, S. A., Patil, S. B., Uzair, M., Fang, J., Zhao, J., Guo, T.,…Li, X. (2020). DEGENERATED PANICLE AND PARTIAL STERILITY 1 (DPS1) encodes a cystathionine beta-synthase domain containing protein required for anther cuticle and panicle development in rice. *New Phytologist*, 225(1), 356–375. https://doi.org/10.1111/nph.16133.

Zhang, H., Li, J., Yoo, J. H., Yoo, S. C., Cho, S. H., Koh, H. J., Seo, H. S., & Paek, N-C. (2006). Rice Chlorina-1 and Chlorina-9 encode ChlD and ChlI subunits of Mg-chelatase, a key enzyme for chlorophyll synthesis and chloroplast development. *Plant Molecular Biology*, 62(3), 325–337. https://doi.org/10.1007/s11103-006-9024-z.

Zhao, G., Shi, J., Liang, W., Xue, F., Luo, Q., Zhu, L.,…Zhang, D. (2015). Two ATP binding cassette G transporters, rice ATP binding Cassette G26 and ATP binding Cassette G15, collaboratively regulate rice male reproduction. *Plant Physiology*, 169(3), 2064–2079. https://doi.org/10.1104/pp.15.00262.

Zhao, J., Zhao, L., Zhang, M., Zafar, S. A., Fang, J., Li, M., Zhang, W., & Li, X. (2017). Arabidopsis E3 ubiquitin ligases PUB22 and PUB23 negatively regulate drought tolerance by targeting ABA receptor PYL9 for degradation. *International Journal of Molecular Sciences*, 18(9), 1841.

Zhao, Q., Zhou, L., Liu, J., Du, X., Asad, M. A., Huang, F., Pan, G., & Cheng, F. (2018). Relationship of ROS accumulation and superoxide dismutase isozymes in developing anther with floret fertility of rice under heat stress. *Plant Physiology and Biochemistry*, 122, 90–101. https://doi.org/10.1016/j.plaphy.2017.11.009.

Zheng, S., Li, J., Ma, L., Wang, H., Zhou, H., Ni, E.…Zhuang, C. (2019). OsAGO2 controls ROS production and the initiation of tapetal PCD by epigenetically regulating OsHXK1 expression in rice anthers. *Proceedings of the National Academy of Sciences of the United States of America*, 116(15), 7549–7558. https://doi.org/10.1073/pnas.1817675116.

Zheng, X., Jehanzeb, M., Habiba, Z., Li, L., & Miao, Y. (2019). Characterization of S40-like proteins and their roles in response to environmental cues and leaf senescence in rice. *BMC Plant Biology*, 19(1), 174. https://doi.org/10.1186/s12870-019-1767-1.

SUPPORTING INFORMATION

Additional supporting information may be found online in the Supporting Information section.